Far-infrared, Raman spectroscopy, and microwave dielectric properties of La(Mg0.5Ti(0.5−x)Snx)O3 ceramics

G. Santosh Babu, V. Subramanian, V. R. K. Murthy, I-Nan Lin, Chia-Ta Chia et al.

Citation: J. Appl. Phys. **102**, 064906 (2007); doi: 10.1063/1.2778743
View online: http://dx.doi.org/10.1063/1.2778743
View Table of Contents: http://jap.aip.org/resource/1/JAPIAU/v102/i6
Published by the AIP Publishing LLC.

Far-infrared, Raman spectroscopy, and microwave dielectric properties of $La(Mg_{0.5}Ti_{(0.5-x)}Sn_x)O_3$ ceramics

G. Santosh Babu, V. Subramanian,[a] and V. R. K. Murthy
Department of Physics, Indian Institute of Technology, Madras, Chennai, 600 036, India

I-Nan Lin
Department of Physics, Tamkang University, Tamsui, Taipei, Taiwan 251, Republic of China

Chia-Ta Chia and Hsiang-Lin Liu
Department of Physics, National Taiwan Normal University, Taipei, Taiwan 116, Republic of China

(Received 30 May 2007; accepted 23 July 2007; published online 19 September 2007)

$La(Mg_{0.5}Ti_{(0.5-x)}Sn_x)O_3$ perovskite ceramics with composition ($x=0.0-0.5$) are prepared by the solid state reaction method. The ceramics are characterized by x-ray diffraction, far-infrared reflectance, Raman spectroscopy, and microwave dielectric properties. The symmetry of ceramics is monoclinic with $P2_1/n$ space group. Intrinsic dielectric constant and loss are estimated by fitting reflectance to the four-parameter semiquantum model. Transverse optic phonon mode strengths and average phonon damping are calculated. The modes corresponding to *B*-site ordering are identified in Raman spectra and the A_{1g} mode of $La(MgTi)_{0.5}O_3$ is analyzed by assuming two merging modes. The variation of long-range order is correlated with full width half maximum of the A_{1g} mode. Microwave measurements are carried out in the frequency range of 8–10 GHz. The dielectric constant (ε') is found to gradually decrease from 28.4 to 19.7 with an increase in tin concentration, whereas the temperature coefficient of resonant frequency (τ_f) decreases from −68 to −84 ppm/°C. The product of the quality factor and resonant frequency ($Q\times f$) obtained for $La(MgTi)_{0.5}O_3$ is 55,000 GHz, that decreases to 46,000 for $x=0.25$ composition and then increases to 63,000 GHz for $La(MgSn)_{0.5}O_3$. © *2007 American Institute of Physics*. [DOI: 10.1063/1.2778743]

I. INTRODUCTION

Ceramic dielectrics with high quality factor (Q), high dielectric constant (ε'), and near zero temperature coefficient of resonant frequency (τ_f), termed as dielectric resonators, are extensively used in microwave communication systems. The emerging new technologies, such as global positioning systems, low-temperature co-fired ceramics for embedded microwave circuitry, tunable filters, and high frequency applications, for advanced radar systems combined with cost effectiveness demand new materials and a better understanding of their properties.[1] Recently there has been a growing interest on rare earth based 1:1 *B*-site ordered complex perovskites with the chemical formula $Ln(B'B'')_{0.5}O_3$ (where Ln=La and Nd; B′=Mg, Co, and and Zn; and B″=Ti and Sn) for the production of microwave resonators.[2–6] These materials crystallize with a monoclinic $P2_1/n$ space group due to $a^-a^-c^+$ tilting and *B*-site ordering, exhibit large values of a negative temperature coefficient, a high quality factor, and a moderate dielectric constant. Solid solutions with positive temperature coefficient of resonant frequency materials such as $CaTiO_3$(CT), $BaTiO_3$(BT), $SrTiO_3$(ST), and $La_{2/3}TiO_3$(LT) have been synthesized to compensate for the negative temperature coefficient of resonant frequency.[4,7–10] In this process, the quality factors are reduced, the dielectric constant is improved and the crystal symmetry modified with the disappearance of 1:1 *B*-site ordering.

Microwave dielectric properties are known to depend on chemical ordering, crystal structure, relative density, and microstructure. In particular, dielectric loss at microwave frequencies is contributed by extrinsic and intrinsic losses. The extrinsic losses are caused by porosity, defects, and second phase, whereas the intrinsic losses are related to constituent atoms, the composition, and the crystal structure of the material. According to Tamura,[11] dielectric loss is mainly due to the contribution of anharmonic terms in the crystal potential energy. The anharmonicity is increased by lattice defects such as disordered charge distribution. Petzelt *et al.*[12] concluded that anharmonicity increased with the increase in permittivity and thereby an increase in dielectric loss. The effect of anharmonicity and dielectric losses can be estimated by Fourier transform infrared (FTIR) reflectance spectroscopy. The intrinsic parameters can be determined either by four-parameter semiquantum model or Lorentz model.[6,13,14] However, broad reflectivity bands and overlapping modes are described more accurately by the former model. Infrared reflectivity (IR) is not so sensitive to the details of processing and to small concentration (of the order of 1 wt %) of dopants. The IR active modes corresponding to a $A-BO_6$ vibration are shown to be responsible for the main contribution of dielectric properties in the solid solution of $La(MgTi)_{0.5}O_3$(LMT)$-Nd(MgTi)_{0.5}O_3$(NMT).[6]

A recent review of microwave dielectrics by Reaney and co-workers concluded that the quality factor (Q) is optimized when the spread of the tolerance factor (Δt) is a minimum in solid solutions made of positive and negative temperature

[a]Author to whom all correspondence should be addressed. Electronic mail: manianvs@iitm.ac.in

coefficient perovskites[1] and the short range order (SRO) is detrimental, whereas the long range order (LRO) enhanced Q.[1,15] Sharp and intense Raman active A_{1g} and F_{2g} modes are correlated with a high degree of LRO.[16,17] The Raman spectroscopy technique is also highly sensitive to SRO and offers a means of detection. The F_{2g} mode is only sensitive to LRO but A_{1g} mode is either due to LRO or SRO.[18] SRO induces a distribution of unit cell parameters of the order of a few nanometers; this may result in anharmonicity and phonon damping, thereby reducing Q.[15] Low quality factors of 0.5LMT–0.5CT, 0.5LMT–0.5BT, and 0.5LMT–0.5CT solid solutions are due to the presence of SRO.[1,15] Levin *et al.*[19] observed asymmetric broadening in the A_{1g} mode of LMT and stressed the need to study detailed Raman analysis on solid solutions with varying order parameters to clarify the origin of anomalous broadening.

In this work $La(Mg_{0.5}Ti_{(0.5-x)}Sn_x)O_3$ ($x=0-0.5$) ceramics are chosen, where the end compositions LMT and $La(MgSn)_{0.5}O_3$ (LMS) exhibit the same symmetry of monoclinic $P2_1/n$. This work reports investigation of FTIR reflectance, Raman spectra, x-ray diffraction data, and microwave dielectric properties. Dielectric parameters obtained by extrapolating IR fitting values to microwave frequencies are compared with microwave data and the correlation of phonon modes to dielectric properties is discussed. The effect of LRO on quality factors with varying composition is also analyzed.

II. EXPERIMENT

$La(Mg_{0.5}Ti_{(0.5-x)}Sn_x)O_3$ ($x=0$, 0.125, 0.25, 0.37, and 0.5) powders were prepared by the solid state reaction method by mixing individual high-purity oxides La_2O_3 (Alfa Aesar, 99.99%), MgO (Alfa Aesar, 99.95%), TiO_2 (Alfa Aesar, 99.9%), and SnO_2 (Cerac, 99.9%). The starting materials were weighed stoichiometrically after drying La_2O_3 at 1000 °C for 24 h and MgO at 800 °C for 6 h to remove moisture content and carbonates. The powders were then dry mixed with an agate mortar and pestle and subsequently wet mixed using distilled water medium. The wet mixed powder was dried in an oven at 150 °C for 6 h. Calcination was done with repeated cycles of heating and mixing. Calcination temperature varied between 1200 to 1250 °C. Calcined powder with the organic binder polyvinyl alcohol was pressed into pellets using uniaxial press and the binder was evaporated at 500 °C for 12 h. Sintering was carried out at 1600 °C for 4 h.

X-ray diffraction data were collected using PaNAlytical X'pert pro MPD in Bragg-Brentano geometry with X'celerator detector. The collection conditions were Cu $K\alpha$ radiation, 40 kV 30 mA, 0.017° step scan, 1.0° divergence slit and 0.02 rad incident and receiving soller slits. Densities of the sintered samples were measured using the Archimedes method. The microwave dielectric measurements were carried out using the N5230A vector Network Analyzer. The TE_{011} or $TE_{01\delta}$ mode was used for the measurements. The dielectric constant (ε_r) was measured using the Hakki–Coleman[20] dielectric resonator method as modified and improved by Courtney.[21] The quality factor (Q) was measured using the reflection mode gold coated copper cavity. The temperature coefficient of resonant frequency was measured using a temperature controlled hot plate enclosure with an invar cavity in the temperature range of 30–70 °C.

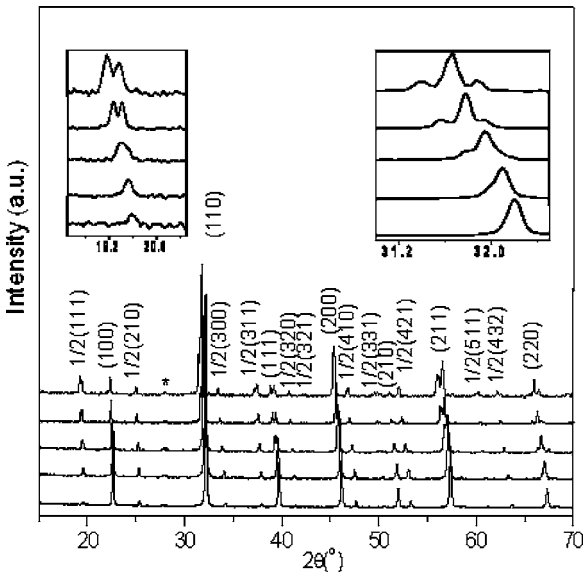

FIG. 1. X-ray diffraction patterns of $La(Mg_{0.5}Ti_{(0.5-x)}Sn_x)O_3$, $x=0.0$ (bottom), 0.125, 0.25, 0.375, and 0.5 (top) ceramics. The impurity peak is shown by the asterisk. The left-hand inset shows (1/2)(111) peak and the right inset shows (110) peak.

The samples were one-side polished using 0.25 μm diamond paste and subsequently annealed at 500 °C for 8 h to remove the residual stress left from the polishing for spectroscopic measurements. Far-infrared and mid-infrared reflectance spectra were obtained using a Bruker IFS 66v FTIR spectrometer. The modulated light beam from the spectrometer was focused onto either the sample or an Au-reference mirror, and the reflected beam was directed onto a 4.2 K bolometer detector (40–600 cm^{-1}) and a B-doped Si photoconductor (450–4000 cm^{-1}). The different sources, beam splitters, and detectors used in these studies provided substantial spectral overlap, and the reflectance mismatch between adjacent spectral ranges was less than 1%. Raman measurements were carried out using a DILOR XY 800 triple-grating Raman spectrometer equipped with a liquid-nitrogen-cooled CCD. The 514.5 nm line of an Ar^+ ion laser with an output 10 mW was used as the excitation source and an Olympus BH-2 microscope with 100× objective was employed for micro-Raman detection. FTIR spectra and the width of A_{1g} mode of Raman spectra were analyzed using FOCUS software.[22] Prior to fitting A_{1g} mode to Lorentzian peak, a base line correction was applied to the experimental data.

III. RESULTS AND DISCUSSION

A. X-ray characterization

Figure 1 displays the x-ray diffraction pattern of $La(Mg_{0.5}Ti_{(0.5-x)}Sn_x)O_3$ ($x=0.0$, 0.125, 0.25, 0.375, and 0.5) ceramics. An unidentified minor impurity peak (less than 2 wt %) is observed in all the patterns. All the reflections shift toward the lower angle, indicating an increase in the

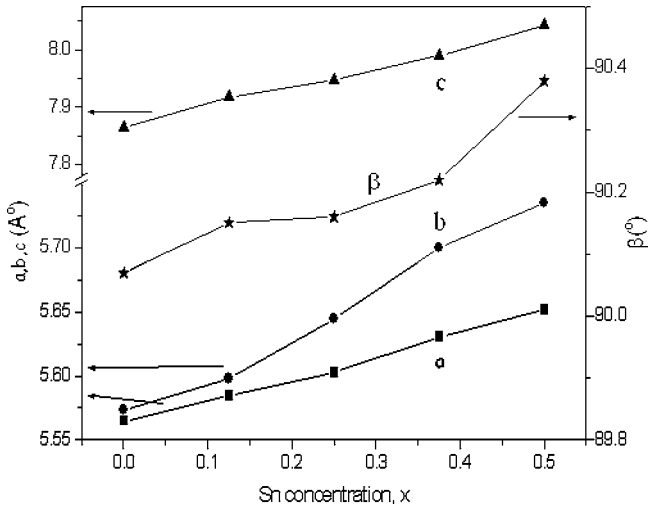

FIG. 2. Lattice parameters as function of Sn content, x (a—squares, b—circles, c—triangles, and β—stars).

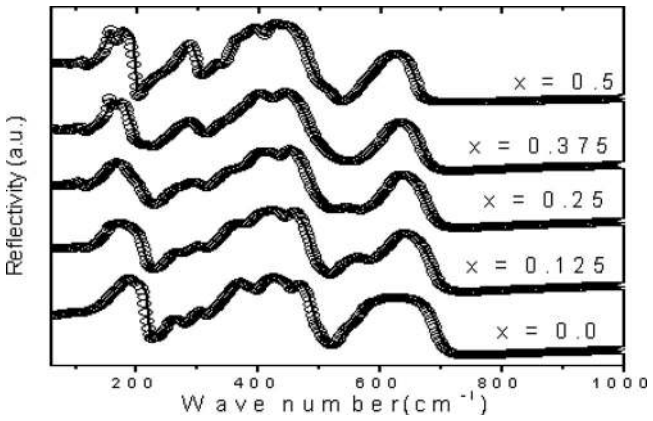

FIG. 3. IR reflectivity spectra of $La(Mg_{0.5}Ti_{(0.5-x)}Sn_x)O_3$ perovskite system (open circles represent the experimental data and continuous line represents the fitted model).

unit cell dimensions with an increase in tin concentration. As mentioned earlier, the symmetry of the end products LMS and LMT are monoclinic $P2_1/n$ space group with $a^-a^-c^+$ tilting.[5,7] The symmetry of the intermediate compositions is examined using WINPLOTR software[23] and found to be monoclinic $P2_1/n$.

The x-ray diffraction patterns are indexed based on cubic perovskite unit cell. Superlattice reflections corresponding to out of phase tilting [(1/2)(311),(1/2)(321),(1/2)(331), and (1/2)(511)], in phase tilting [(1/2)(321)] and anti-parallel displacement of A-cations [(1/2)(210),(1/2)(320),(1/2)×(410),(1/2)(210), and (1/2)(432)] are observed in all the compositions.[24] The (1/2)(111) super lattice reflection usually assigned to 1:1 cation ordering is also observed in all the patterns. The recent work on $La(ZnTi)_{0.5}O_3$(LZT) reveals that the mere presence of (1/2)(111) reflection does not indicate the existence of ordering.[3] The left-hand side inset of Fig. 1 shows variation of (1/2)(111) reflection intensity with an increase in tin concentration. The intensity improvement is assigned to increase in the scattering length difference between B-site cations (scattering length difference between Mg^{+2} and Sn^{+4} is greater than Mg^{+2} and Ti^{+4}), which implies that intensity (1/2)(111) reflection is dependent on B-site cations, therefore suggests the existence of the ordering. However, the symmetry of $P2_1/n$ for all the compositions confirms the existence of 1:1 B-site cation ordering.

The x-ray reflections show splitting with an increase in tin concentration (Fig. 1), and the splitting is highest in LMS. Two insets of Fig. 1 show the evolution of splitting in (1/2)(111) and (110) reflections. The lattice constants of the perovskites are refined using CELREF software (version 3).[25] The increase in lattice parameters along with increase in separation between lattice parameters a and b is observed (Fig. 2).

B. FTIR spectra

The infrared reflectivity spectra of compositions studied are shown in Fig. 3. The reflectivity spectra studies on alkaline earth based perovskites suggest three categories of modes. $A-BO_6$ translation modes in the vicinity of 150 cm^{-1}, B–O–B bonding modes in the range of 200 −400 cm^{-1} and $B-O_6$ bending modes in the range of 500 −800 cm^{-1}.[26] More recent work on LZT suggests that modes between 200 and 500 cm^{-1} are related to cation ordering and octahedral tilting.[27,28] A visual inspection of Fig. 3 indicates that all the spectra appear similar with the presence of three categories of modes, which suggests the same symmetry and presence of B-site ordering in accordance with x-ray diffraction analysis.

According to factor group analysis, the number of IR active modes for $P2_1/n$ symmetry are 33 (17 A_u+16 B_u). Due to anisotropy averaging out in the ceramic samples, modes A_u and B_u cannot be resolved and therefore, the number of effective modes would be 17.[28] In order to evaluate the intrinsic parameters, infrared reflectance spectra are analyzed by fitting the reflectance data to a four-parameter model. Prior to the fitting, transverse optic (TO) and longitudinal optic mode positions for each composition are determined by ε'' and $1/\varepsilon'$ spectra obtained by the Kramers–Kronig inversion. The end compositions LMT and LMS are fitted with 17 modes and the intermediate compositions with x=0.125, 0.25, and 0.375 are fitted with 15, 14, and 14 modes, respectively. The number of modes detected for intermediate compositions are less than 17, due to the broadening of the modes.

The estimated intrinsic values of dielectric constant and quality factor are listed in Table I. The accuracy of these values depends upon the quality of fit to low frequency data. Figure 4 presents TO mode frequencies, strengths and its variations with tin concentration (open circles denote strength of TO modes). The contribution of the vibrations between La and BO_6 to the extrapolated dielectric constant is much higher, followed by a mode in the vicinity of 350 cm^{-1}. It is to be noted that the strength of the modes corresponding to $A-BO_6$ vibrations varies predominantly, even though there is no substitution of ions at A site. The higher contribution of $A-BO_6$ modes to the dielectric constant and loss is in accordance with the study of LMT $-(NaNd)_{0.5}TiO_3$ by Kim *et al.*[29] It is also observed that the

TABLE I. Relative density, dielectric characteristics extrapolated from infrared (IR) data, Lorentzian fit parameters of A_{1g} mode (Raman), and dielectric parameters determined at microwave (MW) frequencies.

		IR		A_{1g} (Raman)		MW	
Tin concentration (x)	Relative density (%)	ε'	$Q\times f$ (GHz)	Shift (cm^{-1})	FWHM (cm^{-1})	ε'	$Q\times f$ (GHz)
0.0	97.2	29.1	85,580	722.2	20.6	28.4	55,000
0.125	97.7	27.0	60,520	713.8	33.0	26.9	50,000
0.25	97.6	24.7	54,860	701.2	36.0	24.4	46,000
0.375	97.4	23.1	70,550	685.1	33.1	22.2	49,000
0.5	98.2	20.5	111,000	668.6	25.1	19.7	63,000

contribution of the mode at 350 cm^{-1} decreases with the increase in tin concentration. This mode might have originated from O−B″−O bending vibrations.

Figure 5 presents the variation of average phonon damping,[30] $\langle\gamma(\mathrm{TO})\rangle$ and intrinsic Q as a function of tin concentration.

$$\langle\gamma(\mathrm{TO})\rangle = \frac{\sum_{j=1}^{n}\gamma_j(\mathrm{TO})\Delta\varepsilon_j}{\sum_{j=1}^{n}\Delta\varepsilon_j}, \quad (1)$$

where γ_j and $\Delta\varepsilon_j$ represent damping and dielectric strength of the TO mode. The intrinsic Q shows a minimum value between $x=0.2$ and 0.25. The average phonon damping shows a peak near $x=0.15$. The close agreement between the intrinsic Q and average phonon damping may be explained by considering the following factors: dielectric constant and the percentage of LRO. The low dielectric constant of LMS compared to LMT should indicate a very low anharmonicity and a very high Q factor compared to LMT,[12] which is not seen due to the low percentage of LRO in LMS (89%) compared to LMT (92%) (Ref. 5) and/or due to the modification of phonon dispersion relations with the substitution of Sn^{+4} having d^{10} electronic configuration. The low Q and correspondingly high phonon damping observed for intermediate compositions may be due to low percentage of LRO, resulting from accommodating three different ions at B site.

C. Raman spectra

Figure 6 presents Raman spectra of $La(Mg_{0.5}Ti_{(0.5-x)}Sn_x)O_3$ ceramics. The Raman spectra of LMT is in good agreement with those reported by Levin *et al.*[10] and Zheng *et al.*[15] It is observed that the modes shift (except modes near 177 and 286 cm^{-1}) to low frequency with increase in tin concentration, attributed to an increase in bond lengths, and thereby a decrease in force constants. The number of Raman active modes for undistorted cubic structure $Fm\bar{3}m$ are $4(A_{1g}+E_g+F_{2g}+F_{1g})$.[16] The factor group analysis predicts 24(12 A_{1g}+12 B_{1g}) active Raman modes for monoclinic $P2_1/n$ space group.[31] It must be noted that for more clarity and an easier analysis, the following discussions are based on the modes of the parent undistorted cubic structure $Fm\bar{3}m$. The mode observed at the highest wave number (approximately 700 cm^{-1}) is assigned to A_{1g} vibrations.[10,15] There exists some ambiguity with respect to the identification of F_{2g} mode and E_g mode in LMT. By analyzing LMT–LT solid solutions,[10] Levin *et al.* related modes at 139

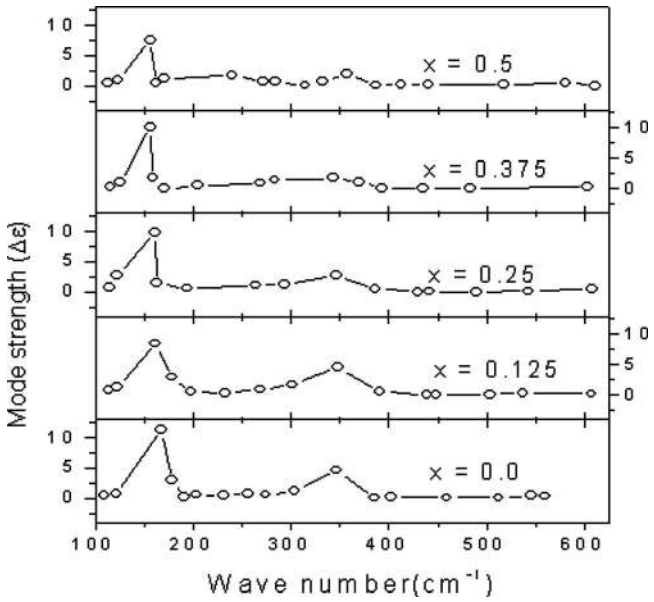

FIG. 4. The variation of TO mode phonon strength as function of Sn concentration, x (open circles represent TO modes).

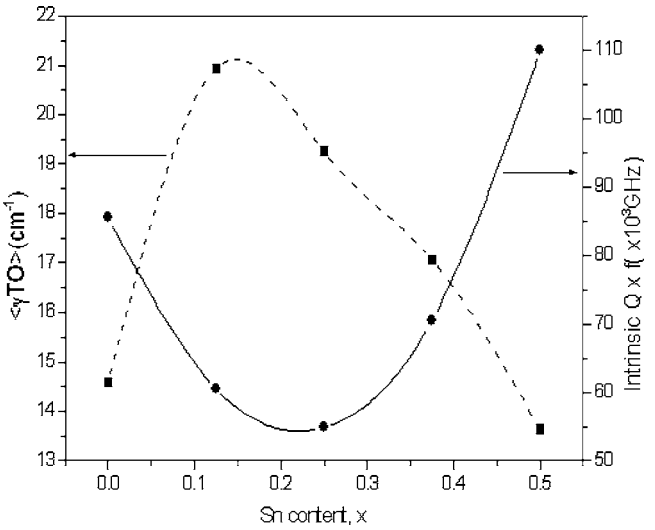

FIG. 5. Intrinsic $Q\times f$ values (circles) and average TO phonon damping (squares) as function of Sn content, x.

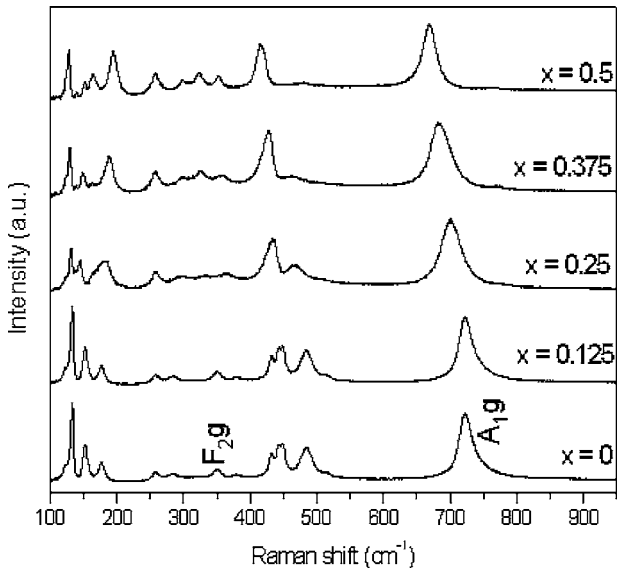

FIG. 6. Raman spectra of $La(Mg_{0.5}Ti_{(0.5-x)}Sn_x)O_3$ system

and 449 cm^{-1} to F_{2g} like vibrations, modes at 437 and 454 cm^{-1} are attributed to octahedral tilting and mode at 491 cm^{-1} due to E_g like vibrations, whereas Zheng *et al.*[15] assigned mode at 353 cm^{-1} to the F_{2g} vibrations in comparison with the spectra of $Pb(ScTa)_{0.5}O_3$.

The presence of F_{2g} mode indicates the existence of LRO, and the FWHM of A_{1g} mode gives the percentage of LRO. The FWHM of A_{1g} mode indicates the degree of SRO in the absence of LRO.[15] It is seen that the intensity of the mode at the vicinity of 353 cm^{-1} initially decreases with the increase in tin content and then increases (Fig. 6). The intensity is minimum in the case of $x=0.25$, indicating a lower percentage of ordering, in accordance with IR analysis. Therefore the present analysis supports that the mode at 353 cm^{-1} originates from F_{2g} like vibrations. Blasse *et al.*[32] reported the absence of E_g mode in LMT and ascribed it to the d^0 configuration of titanium. It is seen from Fig. 6 that the intensity of the mode at 491 cm^{-1} gradually decreases with increase in tin concentration, inferring that it is dependent on tin concentration. Therefore, this mode may not be due to E_g type vibrations. The mode at 139 cm^{-1} is also assigned to F_{2g} type vibrations and its presence is observed in all the compositions. The presence of F_{2g} modes confirms the existence of LRO in all compositions.

A visual inspection of Fig. 6 reveals that A_{1g} mode of LMT is broader with asymmetry compared to LMS. Asymmetric broadening was also observed in LMT by Levin *et al.*[10] A similar asymmetric broadening of A_{1g} mode is found in other titanium based LZT, $Nd(ZnTi)_{0.5}O_3$ (NMT) perovskites and a splitting of A_{1g} mode is observed in $Nd(ZnTi)_{0.5}O_3$ (NZT) perovskite.[33,34] However, a sharp symmetric A_{1g} mode is observed in other tin based $La_xNd_{(1-x)}(MgSn)_{0.5}O_3$ compounds.[34] Therefore, it may be concluded that the presence of titanium results in an asymmetric A_{1g} mode. The broadness of LMT [full-width at half-maximum (FWHM) 27.1 cm^{-1}] reveals that it has a lower percentage of LRO than LMS (FWHM 25.1 cm^{-1}). This also agrees with the earlier work on LMT and LMS by Macke and

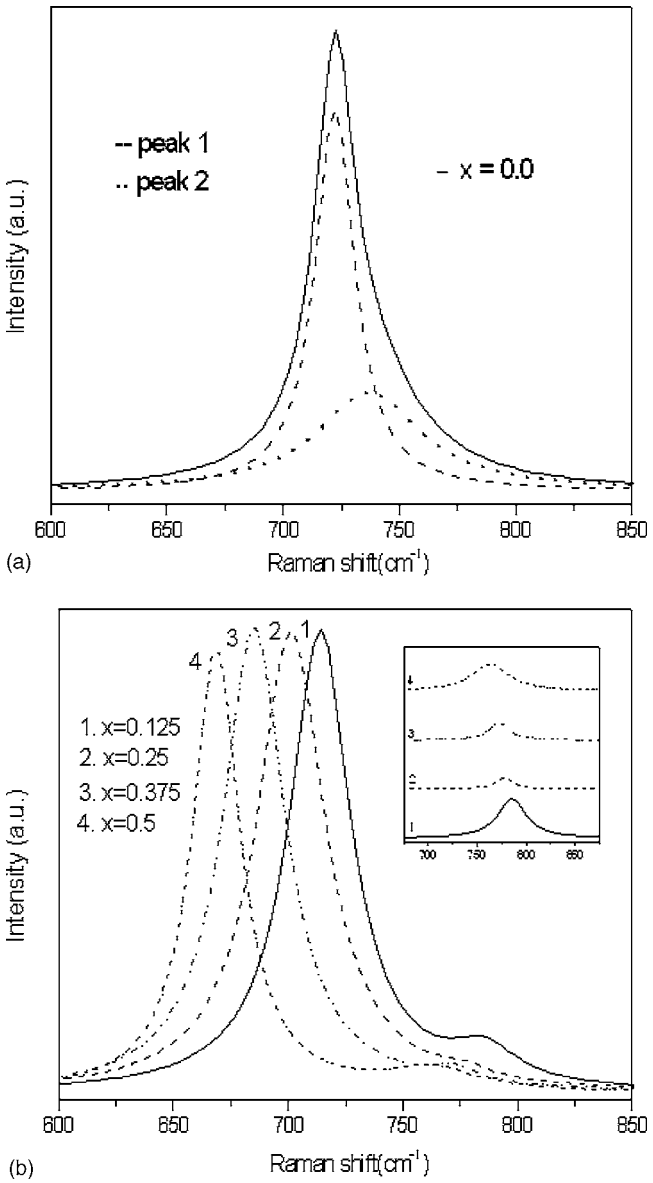

FIG. 7. (a) A_{1g} mode of LMT (solid line) and fit to two peaks (broken and dotted lines).and (b) A_{1g} mode of $La(Mg_{0.5}Ti_{(0.5-x)}Sn_x)O_3$ ceramics, $x=0.125-0.5$. Inset shows weak satellite peak

Blasse,[35] but the difference in ionic radii of Mg^{+2} and Ti^{+4} is high compared to Mg^{+2} and Sn^{+4}, which favor high percentage of LRO in LMT,[5] and the same is confirmed by Rietveld refinement.[5,7] Therefore, there is a discrepancy between the Rietveld refinement and the Raman spectra.

To analyze this further, we have fitted the asymmetric A_{1g} mode of LMT to two Lorentzians. Figure 7(a) shows a symmetric A_{1g} mode at 722.2 cm^{-1} (FWHM 20.6 cm^{-1}) followed by a weak satellite peak at higher frequency (737 cm^{-1}). A weak satellite peak is also observed in other compositions [inset of Fig. 7(b)]. The variation of FWHM of A_{1g} mode with tin concentration is presented in Table I. As the FWHM of A_{1g} mode of LMT (20.6 cm^{-1}) is less than that of LMS (25.1 cm^{-1}), it is clear that the LMT has more percentage of LRO as suggested by Rietveld refinement. Therefore, one has to be more careful in analyzing the asymmetric A_{1g} mode to bring out the nature of ordering. The

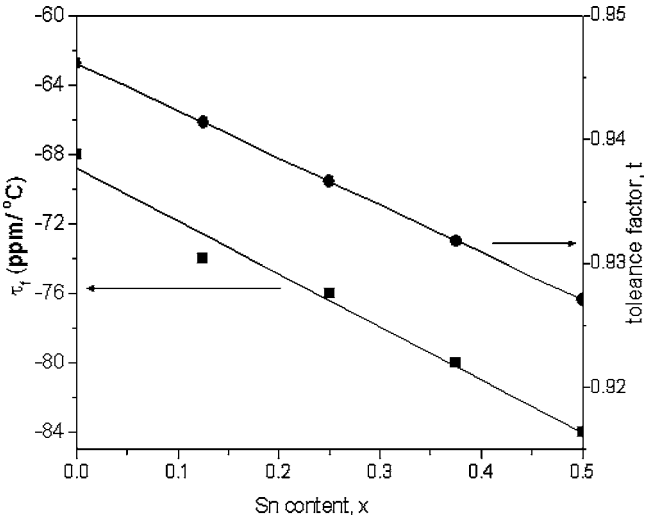

FIG. 8. Tolerance factor (squares) and temperature coefficient of resonant frequency (circles) as functions of Sn concentration, x.

FWHM is maximum at $x=0.25$ composition, which confirms the lowest percentage of ordering as suggested by IR analysis. It was reported that distortions in $B''O_6$ resulted in a number of peaks at A_{1g} mode.[36] Therefore, to understand the reason behind the appearance of extra peaks near the A_{1g} mode, accurate determination of octahedra distortion by estimating bond lengths with neutron diffraction and first principle calculations are warranted.

D. Microwave dielectric properties

Relative density, dielectric constant and quality factors of $La(Mg_{0.5}Ti_{(0.5-x)}Sn_x)O_3$ system are presented in Table I. The dielectric constant decreases with the increase in tin concentration owing to the low ionic polarizability of tin compared to titanium. The quality factors obtained are less than intrinsic values, which is often observed due to the contribution of extrinsic losses. $Q\times f$ values of LMT were reported to be 48,000 GHz by Kipkoech *et al.*,[37] 68,000 GHz by Kim *et al.*,[29] and 114,000 GHz by Seabra *et al.*[6] In the later case, powders were prepared by the pechini method and in the former cases, ball milling was used for mixing, which indicate that $Q\times f$ values depend upon method of preparation. In this study, the quality factor of LMT obtained is 55,000 GHz. It is seen that higher the FWHM of A_{1g} mode lower the $Q\times f$. The trend of $Q\times f$ variation is also in agreement with the IR analysis.

The variation of temperature coefficient of resonant frequency (τ_f) and tolerance factor with tin concentration is presented in Fig. 8. The temperature coefficient of resonant frequency is negative due to the presence of in-phase and anti-phase tilting of octahedra[38] and decreases with the decrease in tolerance factor. This can be explained by an argument that in the tilted region, the increase in thermal energy is completely absorbed to recover the tilting.[29] However, the temperature coefficient of resonant frequency of NMT is reported to be −47 ppm/°C.[6,34] Even though the tolerance factor of NMT (0.916) is less than that of LMT (0.946), its temperature coefficient of resonant frequency is less negative. Further analysis with the calculation of bond valences is in progress.

IV. CONCLUSIONS

The perovskite system $La(Mg_{0.5}Ti_{(0.5-x)}Sn_x)O_3$ $(x=0.0-0.5)$ was prepared by the solid state reaction method. An x-ray diffraction analysis confirmed B-site cation ordering and monoclinic $P2_1/n$ symmetry. The unit cell dimensions increased with the increase in tin content. The modes corresponding to B–O–B bonding vibrations indicating LRO was found in all the compositions and the broadening of modes were seen in intermediate compositions. The variation of mode strengths and the average TO phonon mode damping as a function of tin concentration have been discussed. The intrinsic quality factor is found to correlate with the average phonon damping. The combined study of IR and Raman spectroscopy revealed that intermediate compositions ($x=0.125$, 0.25, and 0.375) exhibit a lower percentage of LRO. The behavior of $Q\times f$ variation is explained by using IR and Raman spectroscopy.

ACKNOWLEDGMENTS

One of the authors (G.S.B.), acknowledges the Council of Scientific and Industrial Research (CSIR), New Delhi, for providing the financial assistance in the form of Senior Research Fellowship. The authors would also like to thank Dr. A. N. Salak for the helpful discussions on IR analysis.

[1] I. M. Reaney and D. Iddles, J. Am. Ceram. Soc. **89**, 2063 (2006).
[2] M. P. Seabra, V. M. Ferreira, H. Zheng, and I. M. Reaney, J. Appl. Phys. **97**, 033525 (2005).
[3] R. Ubic,Y. Hu, and I. Abrahams, Acta Crystallogr., Sect. B: Struct. Sci. **62**, 521 (2006).
[4] A. N. Salak, D. D. Khalyavin, V. M. Ferreira, J. L. Ribeiro, and L. G. Vieira, J. Appl. Phys. **99**, 094104 (2006).
[5] G. Santosh Babu, V. Subramanian, and V. R. K. Murthy, J. Eur. Ceram. Soc. **27**, 2973 (2007).
[6] M. P. Seabra, A. N. Salak, M. Avdeev, and V. M. Ferreira, J. Phys.: Condens. Matter **15**, 4229 (2003).
[7] M. V. Avdeev, M. P. Seabra, and V. M. Ferreira, J. Mater. Res. **17**, 1112 (2002).
[8] M. V. Avdeev, M. P. Seabra, and V. M. Ferreira, Mater. Res. Bull. **37**, 1459 (2002).
[9] A. N. Salak, D. D. Khalyavin, P. Q. Mantas, A. M. R. Senos, and V. M. Ferreira, J. Appl. Phys. **98**, 034101 (2005).
[10] I. Levin, T. A. Vanderrah, T. G. Amos, and J. E. Malsar, Chem. Mater. **17**, 3273 (2005).
[11] H. Tamura, J. Eur. Ceram. Soc. **26**, 1775 (2006).
[12] J. Petzelt and S. Kamba, Ferroelectrics **176**, 145 (1996).
[13] Y. C. Chen, H. F. Cheng, H. L. Liu, C. T. Chia, and I. N. Lin, J. Appl. Phys. **94**, 3365 (2003).
[14] J. Venkatesh, V. Sivasubramanian, V. Subramanian, and V. R. K. Murthy, Mater. Res. Bull. **35**, 1325 (2000).
[15] H. Zheng, I. M. Reaney, G. D. C. Csete de Gyorgyfalva, R. Ubic, J.Yarwood, M. P. Seabra, and V. M. Ferreira, J. Mater. Res. **19**, 488 (2004).
[16] D. Rout, V. Subramanian, K. Hariharan, V. R. K. Murthy, and V. Sivasubramanian, J. Appl. Phys. **98**, 103503 (2005).
[17] N. Setter and I. Laulicht, Appl. Spectrosc. **41**, 526 (1987).
[18] I. M. Reaney, Y. Iqbal, H. Zheng, H. Hughes, D. Iddles, D. Muir, and T. Price, J. Eur. Ceram. Soc. **25**, 1183 (2005).
[19] I. Levin, S. A. Prosandeev, and J. E. Maslar, Appl. Phys. Lett. **86**, 011919 (2005).
[20] B. W. Hakki and P. D. Coleman, IRE Trans. Microwave Theory Tech. **8**, 402 (1960).

[21]W. E. Courtney, IEEE Trans. Microw. Theory Tech. **18**, 476 (1970).
[22]D. De Sousa Meneses, G. Gruener, M. Malki, and P. Echegut, J. Non-Cryst. Solids **351**, 124 (2005).
[23]T. Roisnel and J. Rodriguez-Carvajal, Mater. Sci. Forum **378–381**, 118 (2000).
[24]A. M. Glazer, Acta Crystallogr., Sect. A: Cryst. Phys., Diffr., Theor. Gen. Crystallogr. **31**, 756 (1975).
[25]U. D. Altermatt and I. D. Brown, Acta Crystallogr., Sect. A: Found. Crystallogr. **43**, 125 (1987).
[26]M. Furuya, J. Appl. Phys. **85**, 1084 (1999).
[27]S. Y. Cho, H. J. Yoon, H. J. Lee, and K. S. Hong, J. Am. Ceram. Soc. **84**, 753 (2001).
[28]A. N. Salak, M. P. Seabra, V. M. Ferreira, J. L. Ribeiro, and L. G. Vieira, J. Phys. D **37**, 914 (2004).
[29]J. B. Kim, K. H. Yoon, Y. S. Cho, W. S. Kim, and E. S. Kim, J. Am. Ceram. Soc. **88**, 612 (2005).
[30]M. P. Seabra, A. N. Salak, V. M. Ferreira, J. L. Ribeiro, and L. G. Vieira, J. Eur. Ceram. Soc. **24**, 2995 (2004).
[31]E. Cockayne, J. Appl. Phys. **90**, 1459 (2001).
[32]G. Blasse and A. F. Corsmit, J. Solid State Chem. **6**, 513 (1973).
[33]R. Ubic, K. Khamoushi, D. Iddles, and T. Price, Ceram. Trans. **167**, 21 (2005).
[34]G. Santosh Babu, V. Subramanian and V. R. K. Murthy (to be published).
[35]A. J. H. Macke and G. Blasse, J. Inorg. Nucl. Chem. **38**, 1407 (1976).
[36]V. V. Fomichev, Russ. Chem. Bull. **43**, 1943 (1994).
[37]E. R. Kipkoech, F. Azough, and R. Freer, J. Appl. Phys. **97**, 064103 (2005).
[38]I. M. Reaney, E. L. Colla, and N. Setter, Jpn. J. Appl. Phys. **33**, 3984 (1994).